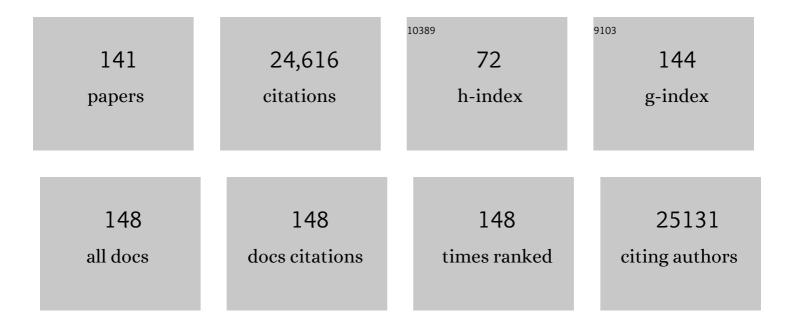
List of Publications by Year in descending order

Source: https://exaly.com/author-pdf/2382020/publications.pdf Version: 2024-02-01



SHUL-RIN YANC

| # | Article | IF | CITATIONS |
|----|---|------|-----------|
| 1 | Harnessing the Unique Features of 2D Materials toward Dendriteâ€free Metal Anodes. Energy and Environmental Materials, 2022, 5, 45-67. | 12.8 | 33 |
| 2 | Efficient polysulfides conversion on Mo2CTx MXene for high-performance lithium–sulfur batteries. Rare Metals, 2022, 41, 311-318. | 7.1 | 40 |
| 3 | Single-Atom Pt Anchored on Oxygen Vacancy of Monolayer Ti ₃ C ₂ T _{<i>x</i>} for Superior Hydrogen Evolution. Nano Letters, 2022, 22, 1398-1405. | 9.1 | 76 |
| 4 | Singleâ€Atom Reversible Lithiophilic Sites toward Stable Lithium Anodes. Advanced Energy Materials, 2022, 12, . | 19.5 | 49 |
| 5 | Chargeâ€Enriched Strategy Based on MXeneâ€Based PolypyrroleÂLayers Toward Dendriteâ€Free Zinc Metal Anodes. Advanced Energy Materials, 2022, 12, . | 19.5 | 108 |
| 6 | A perspective on highâ€entropy twoâ€dimensional materials. SusMat, 2022, 2, 65-75. | 14.9 | 19 |
| 7 | A Highly Durable Rubberâ€Derived Lithiumâ€Conducting Elastomer for Lithium Metal Batteries. Advanced Science, 2022, 9, e2200553. | 11.2 | 22 |
| 8 | Vertically Aligned MXene Nanosheet Arrays for Highâ€Rate Lithium Metal Anodes. Advanced Energy Materials, 2022, 12, . | 19.5 | 61 |
| 9 | Stressâ€Release Functional Liquid Metalâ€MXene Layers toward Dendriteâ€Free Zinc Metal Anodes. Advanced Energy Materials, 2022, 12, . | 19.5 | 58 |
| 10 | Highâ€Entropy Carbonitride MAX Phases and Their Derivative MXenes. Advanced Energy Materials, 2022, 12, . | 19.5 | 69 |
| 11 | Formation of Superâ€Assembled TiO _{<i>x</i>} /Zn/Nâ€Doped Carbon Inverse Opal Towards Dendriteâ€Free Zn Anodes. Angewandte Chemie - International Edition, 2022, 61, e202115649. | 13.8 | 76 |
| 12 | Formation of Superâ€Assembled TiO _{<i>x</i>} /Zn/Nâ€Doped Carbon Inverse Opal Towards Dendriteâ€Free Zn Anodes. Angewandte Chemie, 2022, 134, . | 2.0 | 4 |
| 13 | 2D Nonâ€Van Der Waals Transitionâ€Metal Chalcogenide Layers Derived from Vanadiumâ€Based MAX Phase for Ultrafast Zinc Storage. Advanced Energy Materials, 2022, 12, . | 19.5 | 8 |
| 14 | Lowâ€Tortuous MXene (TiNbC) Accordion Arrays Enabled Fast Ion Diffusion and Charge Transfer in Dendriteâ€Free Lithium Metal Anodes. Advanced Energy Materials, 2022, 12, . | 19.5 | 14 |
| 15 | Boron-doping induced lithophilic transition of graphene for dendrite-free lithium growth. Journal of Energy Chemistry, 2021, 56, 463-469. | 12.9 | 18 |
| 16 | 3D Printing Lithium Salt towards Dendrite-free Lithium Anodes. Energy Storage Materials, 2021, 35, 108-113. | 18.0 | 21 |
| 17 | Selective Etching Quaternary MAX Phase toward Single Atom Copper Immobilized MXene (Ti ₃ C ₂ Cl _{<i>x</i>) for Efficient CO₂ Electroreduction to Methanol. ACS Nano, 2021, 15, 4927-4936.} | 14.6 | 139 |
| 18 | Tortuosity Modulation toward Highâ€Energy and Highâ€Power Lithium Metal Batteries. Advanced Energy Materials, 2021, 11, 2003663. | 19.5 | 46 |

| # | Article | IF | CITATIONS |
|----|---|------|-----------|
| 19 | Creating New Battery Configuration Associated with the Functions of Primary and Rechargeable Lithium Metal Batteries. Advanced Energy Materials, 2021, 11, 2003746. | 19.5 | 19 |
| 20 | Ultrafast Zinc–Ion–Conductor Interface toward Highâ€Rate and Stable Zinc Metal Batteries. Advanced Energy Materials, 2021, 11, 2100186. | 19.5 | 223 |
| 21 | Interlamellar Lithiumâ€ion Conductor Reformed Interface for High Performance Lithium Metal Anode. Advanced Functional Materials, 2021, 31, 2102336. | 14.9 | 23 |
| 22 | Rücktitelbild: Tricycloquinazolineâ€Based 2D Conductive Metal–Organic Frameworks as Promising Electrocatalysts for CO ₂ Reduction (Angew. Chem. 26/2021). Angewandte Chemie, 2021, 133, 14840-14840. | 2.0 | 0 |
| 23 | Tricycloquinazolineâ€Based 2D Conductive Metal–Organic Frameworks as Promising Electrocatalysts for CO ₂ Reduction. Angewandte Chemie - International Edition, 2021, 60, 14473-14479. | 13.8 | 130 |
| 24 | Tricycloquinazolineâ€Based 2D Conductive Metal–Organic Frameworks as Promising Electrocatalysts for CO 2 Reduction. Angewandte Chemie, 2021, 133, 14594-14600. | 2.0 | 12 |
| 25 | Singleâ€Atom Sites on MXenes for Energy Conversion and Storage. Small Science, 2021, 1, 2100017. | 9.9 | 48 |
| 26 | Nitrogenâ€Doped Porous Carbon Nanosheets with Ultrahigh Capacity and Quasicapacitive Energy Storage Performance for Lithium and Sodium Storage Applications. Energy Technology, 2021, 9, 2100309. | 3.8 | 4 |
| 27 | Highâ€Entropy Atomic Layers of Transitionâ€Metal Carbides (MXenes). Advanced Materials, 2021, 33, e2101473. | 21.0 | 122 |
| 28 | Nano high-entropy alloy with strong affinity driving fast polysulfide conversion towards stable lithium sulfur batteries. Energy Storage Materials, 2021, 43, 212-220. | 18.0 | 65 |
| 29 | High-Throughput Production of 1T MoS ₂ Monolayers Based on Controllable Conversion of Mo-Based MXenes. ACS Nano, 2021, 15, 19275-19283. | 14.6 | 32 |
| 30 | 3D printing dendrite-free lithium anodes based on the nucleated MXene arrays. Energy Storage Materials, 2020, 24, 670-675. | 18.0 | 82 |
| 31 | Perpendicular MXene Arrays with Periodic Interspaces toward Dendriteâ€Free Lithium Metal Anodes with Highâ€Rate Capabilities. Advanced Functional Materials, 2020, 30, 1908075. | 14.9 | 68 |
| 32 | Ultrathin bismuth nanosheets as an efficient polysulfide catalyst for high performance lithium–sulfur batteries. Journal of Materials Chemistry A, 2020, 8, 149-157. | 10.3 | 43 |
| 33 | Single Zinc Atoms Immobilized on MXene (Ti ₃ C ₂ Cl _{<i>x</i>}) Layers toward Dendrite-Free Lithium Metal Anodes. ACS Nano, 2020, 14, 891-898. | 14.6 | 174 |
| 34 | Harnessing the unique features of MXenes for sulfur cathodes. Tungsten, 2020, 2, 162-175. | 4.8 | 25 |
| 35 | Conversion of Intercalated MoO ₃ to Multiâ€Heteroatomsâ€Doped MoS ₂ with High Hydrogen Evolution Activity. Advanced Materials, 2020, 32, e2001167. | 21.0 | 82 |
| 36 | Catalytic Conversion of Polysulfides on Single Atom Zinc Implanted MXene toward Highâ€Rate Lithium–Sulfur Batteries. Advanced Functional Materials, 2020, 30, 2002471. | 14.9 | 158 |

SHU-BIN YANG

| # | Article | IF | CITATIONS |
|----|--|------|-----------|
| 37 | In Situ Generation of Artificial Solidâ€Electrolyte Interphases on 3D Conducting Scaffolds for Highâ€Performance Lithiumâ€Metal Anodes. Advanced Energy Materials, 2020, 10, 1903339. | 19.5 | 107 |
| 38 | MXeneâ€Based Mesoporous Nanosheets Toward Superior Lithium Ion Conductors. Advanced Energy Materials, 2020, 10, 1903534. | 19.5 | 97 |
| 39 | Conversion of non-van der Waals solids to 2D transition-metal chalcogenides. Nature, 2020, 577, 492-496. | 27.8 | 145 |
| 40 | Vanadium carbide with periodic anionic vacancies for effective electrocatalytic nitrogen reduction. Materials Today, 2020, 40, 18-25. | 14.2 | 34 |
| 41 | Zinc anode with artificial solid electrolyte interface for dendrite-free Ni-Zn secondary battery. Journal of Colloid and Interface Science, 2019, 555, 174-179. | 9.4 | 25 |
| 42 | Endowing the Lithium Metal Surface with Self-Healing Property via an in Situ Gas–Solid Reaction for High-Performance Lithium Metal Batteries. ACS Applied Materials & Interfaces, 2019, 11, 28878-28884. | 8.0 | 24 |
| 43 | Unlocking the Potential of Disordered Rocksalts for Aqueous Zincâ€kon Batteries. Advanced Materials, 2019, 31, e1904369. | 21.0 | 171 |
| 44 | Gradientâ€Distributed Nucleation Seeds on Conductive Host for a Dendriteâ€Free and Highâ€Rate Lithium Metal Anode. Small, 2019, 15, e1903520. | 10.0 | 83 |
| 45 | Rapid and Lowâ€Temperature Saltâ€Templated Production of 2D Metal Oxide/Oxychloride/Hydroxide. Small, 2019, 15, e1904587. | 10.0 | 17 |
| 46 | An artificial TiO ₂ /lithium <i>n</i> -butoxide hybrid SEI layer with facilitated lithium-ion transportation ability for stable lithium anodes. Nanoscale, 2019, 11, 2194-2201. | 5.6 | 43 |
| 47 | A liquid metal-based self-adaptive sulfur–gallium composite for long-cycling lithium–sulfur batteries. Nanoscale, 2019, 11, 412-417. | 5.6 | 29 |
| 48 | Horizontal Growth of Lithium on Parallelly Aligned MXene Layers towards Dendriteâ€Free Metallic Lithium Anodes. Advanced Materials, 2019, 31, e1901820. | 21.0 | 174 |
| 49 | Synergistic electrocatalysis of polysulfides by a nanostructured VS ₄ -carbon nanofiber functional separator for high-performance lithium–sulfur batteries. Journal of Materials Chemistry A, 2019, 7, 16812-16820. | 10.3 | 105 |
| 50 | Dendriteâ€Free Lithium Anodes with Ultraâ€Deep Stripping and Plating Properties Based on Vertically Oriented Lithium–Copper–Lithium Arrays. Advanced Materials, 2019, 31, e1901310. | 21.0 | 112 |
| 51 | A linear molecule sulfur-rich organic cathode material for high performance lithium–sulfur batteries. Journal of Power Sources, 2019, 430, 210-217. | 7.8 | 31 |
| 52 | Room-temperature sodium thermal reaction towards electrochemically active metals for lithium storage. Journal of Colloid and Interface Science, 2019, 551, 10-15. | 9.4 | 3 |
| 53 | Facile fabrication of 2D stanene nanosheets <i>via</i> a dealloying strategy for potassium storage. Chemical Communications, 2019, 55, 3983-3986. | 4.1 | 17 |
| 54 | Few-layer tin–antimony nanosheets: a novel 2D alloy for superior lithium storage. Chemical Communications, 2019, 55, 3975-3978. | 4.1 | 8 |

| # | Article | IF | CITATIONS |
|----|--|------|-----------|
| 55 | Homogeneous guiding deposition of sodium through main group II metals toward dendrite-free sodium anodes. Science Advances, 2019, 5, eaau6264. | 10.3 | 130 |
| 56 | Harnessing the unique properties of 2D materials for advanced lithium–sulfur batteries. Nanoscale Horizons, 2019, 4, 77-98. | 8.0 | 79 |
| 57 | Tin Intercalated Ultrathin MoO ₃ Nanoribbons for Advanced Lithium–Sulfur Batteries. Advanced Energy Materials, 2019, 9, 1803137. | 19.5 | 126 |
| 58 | W-doped VO2(B) nanosheets-built 3D networks for fast lithium storage at high temperatures. Electrochimica Acta, 2019, 295, 393-400. | 5.2 | 26 |
| 59 | Fast Cryomediated Dynamic Equilibrium Hydrolysates towards Grain Boundary-Enriched Platinum Scaffolds for Efficient Methanol Oxidation. Research, 2019, 2019, 8174314. | 5.7 | 5 |
| 60 | 3D Printing Quasiâ€Solidâ€State Asymmetric Microâ€Supercapacitors with Ultrahigh Areal Energy Density. Advanced Energy Materials, 2018, 8, 1800408. | 19.5 | 268 |
| 61 | Mesoporous Hybrid Electrolyte for Simultaneously Inhibiting Lithium Dendrites and Polysulfide Shuttle in Li–S Batteries. Advanced Energy Materials, 2018, 8, 1703124. | 19.5 | 42 |
| 62 | Atomic Layers of MoO ₂ with Exposed Highâ€Energy (010) Facets for Efficient Oxygen Reduction. Small, 2018, 14, e1703960. | 10.0 | 22 |
| 63 | A Material Perspective of Rechargeable Metallic Lithium Anodes. Advanced Energy Materials, 2018, 8, 1702296. | 19.5 | 95 |
| 64 | Vertically oriented growth of MoO ₃ nanosheets on graphene for superior lithium storage. Journal of Materials Chemistry A, 2018, 6, 672-679. | 10.3 | 35 |
| 65 | Ultrathin two-dimensional metallic nanomaterials. Materials Chemistry Frontiers, 2018, 2, 456-467. | 5.9 | 73 |
| 66 | Dendriteâ€Free Metallic Lithium in Lithiophilic Carbonized Metal–Organic Frameworks. Advanced Energy Materials, 2018, 8, 1703505. | 19.5 | 144 |
| 67 | Synergic antimony–niobium pentoxide nanomeshes for high-rate sodium storage. Journal of Materials Chemistry A, 2018, 6, 6225-6232. | 10.3 | 22 |
| 68 | Defect-rich, boron-nitrogen bonds-free and dual-doped graphenes for highly efficient oxygen reduction reaction. Journal of Colloid and Interface Science, 2018, 521, 11-16. | 9.4 | 13 |
| 69 | 3D Printing Sulfur Copolymerâ€Graphene Architectures for Li‧ Batteries. Advanced Energy Materials, 2018, 8, 1701527. | 19.5 | 196 |
| 70 | Two-dimensional nanosheets as building blocks to construct three-dimensional structures for lithium storage. Journal of Energy Chemistry, 2018, 27, 128-145. | 12.9 | 23 |
| 71 | Efficient polysulfide barrier of a graphene aerogel–carbon nanofibers–Ni network for high-energy-density lithium–sulfur batteries with ultrahigh sulfur content. Journal of Materials Chemistry A, 2018, 6, 20926-20938. | 10.3 | 63 |
| 72 | Continuously 3D printed quantum dot-based electrodes for lithium storage with ultrahigh capacities. Journal of Materials Chemistry A, 2018, 6, 19960-19966. | 10.3 | 49 |

| # | Article | IF | CITATIONS |
|----|--|------|-----------|
| 73 | Recent Advances in Synthesis and Applications of 2D Junctions. Small, 2018, 14, e1801606. | 10.0 | 19 |
| 74 | Editorial for rare metals, special issue on solid state batteries. Rare Metals, 2018, 37, 447-448. | 7.1 | 2 |
| 75 | Ultrafast Zn ²⁺ Intercalation and Deintercalation in Vanadium Dioxide. Advanced Materials, 2018, 30, e1800762. | 21.0 | 485 |
| 76 | Ultrastable Inâ€Plane 1T–2H MoS ₂ Heterostructures for Enhanced Hydrogen Evolution Reaction. Advanced Energy Materials, 2018, 8, 1801345. | 19.5 | 409 |
| 77 | V2O3 nanoparticles anchored onto the reduced graphene oxide for superior lithium storage. Electrochimica Acta, 2017, 231, 732-738. | 5.2 | 32 |
| 78 | Multiâ€Atomic Layers of Metallic Aluminum for Ultralong Life Lithium Storage with High Volumetric Capacity. Advanced Functional Materials, 2017, 27, 1700840. | 14.9 | 50 |
| 79 | Liquidâ€Phase Exfoliated Metallic Antimony Nanosheets toward High Volumetric Sodium Storage. Advanced Energy Materials, 2017, 7, 1700447. | 19.5 | 172 |
| 80 | Controllable synthesis of sandwich-like graphene-supported structures for energy storage and conversion. New Carbon Materials, 2017, 32, 1-14. | 6.1 | 13 |
| 81 | Simultaneous Formation of Artificial SEI Film and 3D Host for Stable Metallic Sodium Anodes. ACS Applied Materials & Interfaces, 2017, 9, 40265-40272. | 8.0 | 67 |
| 82 | Two-Dimensional Porous Sandwich-Like C/Si–Graphene–Si/C Nanosheets for Superior Lithium Storage. ACS Applied Materials & Interfaces, 2017, 9, 39371-39379. | 8.0 | 53 |
| 83 | Flexible Ti3C2 MXene-lithium film with lamellar structure for ultrastable metallic lithium anodes. Nano Energy, 2017, 39, 654-661. | 16.0 | 163 |
| 84 | Pre-planted nucleation seeds for rechargeable metallic lithium anodes. Journal of Materials Chemistry A, 2017, 5, 18862-18869. | 10.3 | 28 |
| 85 | 3D-Printed Hierarchical Porous Frameworks for Sodium Storage. ACS Applied Materials & Interfaces, 2017, 9, 41871-41877. | 8.0 | 67 |
| 86 | 3D organic Na ₄ C ₆ O ₆ /graphene architecture for fast sodium storage with ultralong cycle life. Chemical Communications, 2017, 53, 12642-12645. | 4.1 | 19 |
| 87 | Graphene-supported mesoporous titania nanosheets for efficient photodegradation. Journal of Colloid and Interface Science, 2017, 505, 711-718. | 9.4 | 18 |
| 88 | Pyridinicâ€Nitrogenâ€Dominated Graphene Aerogels with Fe–N–C Coordination for Highly Efficient Óxygen Reduction Reaction. Advanced Functional Materials, 2016, 26, 5708-5717. | 14.9 | 360 |
| 89 | A new configured lithiated silicon–sulfur battery built on 3D graphene with superior electrochemical performances. Energy and Environmental Science, 2016, 9, 2025-2030. | 30.8 | 98 |
| 90 | Partially Singleâ€Crystalline Mesoporous Nb ₂ O ₅ Nanosheets in between Graphene for Ultrafast Sodium Storage. Advanced Materials, 2016, 28, 7672-7679. | 21.0 | 171 |

| # | Article | IF | CITATIONS |
|-----|--|------|-----------|
| 91 | Pyridinic Nitrogenâ€Enriched Carbon Nanogears with Thin Teeth for Superior Lithium Storage. Advanced Energy Materials, 2016, 6, 1600917. | 19.5 | 116 |
| 92 | Hybrid 2D–0D Graphene–VN Quantum Dots for Superior Lithium and Sodium Storage. Advanced Energy Materials, 2016, 6, 1502067. | 19.5 | 76 |
| 93 | Copper(<scp>ii</scp>) tungstate nanoflake array films: sacrificial template synthesis, hydrogen treatment, and their application as photoanodes in solar water splitting. Nanoscale, 2016, 8, 5892-5901. | 5.6 | 78 |
| 94 | 3D Reduced Graphene Oxide Coated V ₂ O ₅ Nanoribbon Scaffolds for High-Capacity Supercapacitor Electrodes. Particle and Particle Systems Characterization, 2015, 32, 817-821. | 2.3 | 49 |
| 95 | From Commercial Sponge Toward 3D Graphene–Silicon Networks for Superior Lithium Storage. Advanced Energy Materials, 2015, 5, 1500289. | 19.5 | 114 |
| 96 | Boron- and Nitrogen-Substituted Graphene Nanoribbons as Efficient Catalysts for Oxygen Reduction Reaction. Chemistry of Materials, 2015, 27, 1181-1186. | 6.7 | 219 |
| 97 | 3D Nanostructured Molybdenum Diselenide/Graphene Foam as Anodes for Long-Cycle Life Lithium-ion Batteries. Electrochimica Acta, 2015, 176, 103-111. | 5.2 | 107 |
| 98 | Ultrafine SnO ₂ nanoparticles decorated onto graphene for high performance lithium storage. RSC Advances, 2015, 5, 43798-43804. | 3.6 | 12 |
| 99 | Vertically Aligned Sulfur–Graphene Nanowalls on Substrates for Ultrafast Lithium–Sulfur Batteries. Nano Letters, 2015, 15, 3073-3079. | 9.1 | 183 |
| 100 | Nitrogen-doped holey graphene foams for high-performance lithium storage. RSC Advances, 2015, 5, 91114-91119. | 3.6 | 21 |
| 101 | Nanosized Pt anchored onto 3D nitrogen-doped graphene nanoribbons towards efficient methanol electrooxidation. Journal of Materials Chemistry A, 2015, 3, 19696-19701. | 10.3 | 60 |
| 102 | Fabrication of Fully Fluorinated Graphene Nanosheets Towards Highâ€Performance Lithium Storage. Advanced Materials Interfaces, 2014, 1, 1300149. | 3.7 | 51 |
| 103 | Vertically aligned cobalt oxide nanowires on graphene networks for high-performance lithium storage. Nanotechnology, 2014, 25, 445704. | 2.6 | 10 |
| 104 | Direct chemical conversion of graphene to boron- and nitrogen- and carbon-containing atomic layers. Nature Communications, 2014, 5, 3193. | 12.8 | 198 |
| 105 | CoMoO ₄ Nanoparticles Anchored on Reduced Graphene Oxide Nanocomposites as Anodes for Long-Life Lithium-Ion Batteries. ACS Applied Materials & Interfaces, 2014, 6, 20414-20422. | 8.0 | 125 |
| 106 | Anomalous piezoelectricity in two-dimensional graphene nitride nanosheets. Nature Communications, 2014, 5, 4284. | 12.8 | 228 |
| 107 | Ultrathin single-crystalline vanadium pentoxide nanoribbon constructed 3D networks for superior energy storage. Journal of Materials Chemistry A, 2014, 2, 13136-13142. | 10.3 | 78 |
| 108 | Ptâ€Decorated 3D Architectures Built from Graphene and Graphitic Carbon Nitride Nanosheets as Efficient Methanol Oxidation Catalysts. Advanced Materials, 2014, 26, 5160-5165. | 21.0 | 354 |

SHU-BIN YANG

| # | Article | IF | CITATIONS |
|-----|--|------|-----------|
| 109 | A Bottomâ€Up Approach to Build 3D Architectures from Nanosheets for Superior Lithium Storage. Advanced Functional Materials, 2014, 24, 125-130. | 14.9 | 247 |
| 110 | Use of Organic Precursors and Graphenes in the Controlled Synthesis of Carbon-Containing Nanomaterials for Energy Storage and Conversion. Accounts of Chemical Research, 2013, 46, 116-128. | 15.6 | 158 |
| 111 | Building 3D Structures of Vanadium Pentoxide Nanosheets and Application as Electrodes in Supercapacitors. Nano Letters, 2013, 13, 5408-5413. | 9.1 | 343 |
| 112 | Three-Dimensional Metal–Graphene–Nanotube Multifunctional Hybrid Materials. ACS Nano, 2013, 7, 58-64. | 14.6 | 202 |
| 113 | Grapheneâ€Based Porous Silica Sheets Impregnated with Polyethyleneimine for Superior CO ₂ Capture. Advanced Materials, 2013, 25, 2130-2134. | 21.0 | 140 |
| 114 | Direct Laserâ€Patterned Microâ€Supercapacitors from Paintable MoS ₂ Films. Small, 2013, 9, 2905-2910. | 10.0 | 455 |
| 115 | Bottom-up Approach toward Single-Crystalline VO ₂ -Graphene Ribbons as Cathodes for Ultrafast Lithium Storage. Nano Letters, 2013, 13, 1596-1601. | 9.1 | 263 |
| 116 | 3D Graphene Foams Crossâ€linked with Preâ€encapsulated Fe ₃ O ₄ Nanospheres for Enhanced Lithium Storage. Advanced Materials, 2013, 25, 2909-2914. | 21.0 | 727 |
| 117 | Exfoliated Graphitic Carbon Nitride Nanosheets as Efficient Catalysts for Hydrogen Evolution Under Visible Light. Advanced Materials, 2013, 25, 2452-2456. | 21.0 | 2,227 |
| 118 | Grapheneâ€Networkâ€Backboned Architectures for Highâ€Performance Lithium Storage. Advanced Materials, 2013, 25, 3979-3984. | 21.0 | 253 |
| 119 | Three-Dimensional Graphene-Based Macro- and Mesoporous Frameworks for High-Performance Electrochemical Capacitive Energy Storage. Journal of the American Chemical Society, 2012, 134, 19532-19535. | 13.7 | 1,024 |
| 120 | Hollow carbon spheres with encapsulation of Co3O4 nanoparticles as anode material for lithium ion batteries. Electrochimica Acta, 2012, 78, 440-445. | 5.2 | 54 |
| 121 | Porous Iron Oxide Ribbons Grown on Graphene for High-Performance Lithium Storage. Scientific Reports, 2012, 2, 427. | 3.3 | 119 |
| 122 | Nitrogen-Doped Graphene and Its Iron-Based Composite As Efficient Electrocatalysts for Oxygen Reduction Reaction. ACS Nano, 2012, 6, 9541-9550. | 14.6 | 640 |
| 123 | 3D Nitrogen-Doped Graphene Aerogel-Supported Fe ₃ O ₄ Nanoparticles as Efficient Electrocatalysts for the Oxygen Reduction Reaction. Journal of the American Chemical Society, 2012, 134, 9082-9085. | 13.7 | 1,967 |
| 124 | Efficient Synthesis of Heteroatom (N or S)â€Doped Graphene Based on Ultrathin Graphene Oxideâ€Porous Silica Sheets for Oxygen Reduction Reactions. Advanced Functional Materials, 2012, 22, 3634-3640. | 14.9 | 1,180 |
| 125 | Coplanar Asymmetrical Reduced Graphene Oxide–Titanium Electrodes for Polymer Photodetectors. Advanced Materials, 2012, 24, 1566-1570. | 21.0 | 24 |
| 126 | Sandwichâ€Like, Grapheneâ€Based Titania Nanosheets with High Surface Area for Fast Lithium Storage. Advanced Materials, 2011, 23, 3575-3579. | 21.0 | 503 |

| # | Article | IF | CITATIONS |
|-----|--|------|-----------|
| 127 | 2D Sandwichâ€like Sheets of Iron Oxide Grown on Graphene as High Energy Anode Material for Supercapacitors. Advanced Materials, 2011, 23, 5574-5580. | 21.0 | 526 |
| 128 | Grapheneâ€Based Carbon Nitride Nanosheets as Efficient Metalâ€Free Electrocatalysts for Oxygen Reduction Reactions. Angewandte Chemie - International Edition, 2011, 50, 5339-5343. | 13.8 | 1,024 |
| 129 | Fabrication of Cobalt and Cobalt Oxide/Graphene Composites: Towards Highâ€Performance Anode Materials for Lithium Ion Batteries. ChemSusChem, 2010, 3, 236-239. | 6.8 | 290 |
| 130 | Nanographeneâ€Constructed Hollow Carbon Spheres and Their Favorable Electroactivity with Respect to Lithium Storage. Advanced Materials, 2010, 22, 838-842. | 21.0 | 473 |
| 131 | Grapheneâ€Based Nanosheets with a Sandwich Structure. Angewandte Chemie - International Edition, 2010, 49, 4795-4799. | 13.8 | 457 |
| 132 | Fabrication of Grapheneâ€Encapsulated Oxide Nanoparticles: Towards Highâ€Performance Anode Materials for Lithium Storage. Angewandte Chemie - International Edition, 2010, 49, 8408-8411. | 13.8 | 1,005 |
| 133 | Effect of heat treatment on the morphology and electrochemical performance of TiO2 nanotubes as anode materials for lithium-ion batteries. Materials Chemistry and Physics, 2009, 118, 367-370. | 4.0 | 21 |
| 134 | Carbon nanotube capsules encapsulating SnO2 nanoparticles as an anode material for lithium ion batteries. Electrochimica Acta, 2009, 55, 521-527. | 5.2 | 58 |
| 135 | Carbon-Encapsulated Metal Oxide Hollow Nanoparticles and Metal Oxide Hollow Nanoparticles: A General Synthesis Strategy and Its Application to Lithium-Ion Batteries. Chemistry of Materials, 2009, 21, 2935-2940. | 6.7 | 143 |
| 136 | A comparative study of electrochemical properties of two kinds of carbon nanotubes as anode materials for lithium ion batteries. Electrochimica Acta, 2008, 53, 2238-2244. | 5.2 | 141 |
| 137 | Preparation and electrochemical properties of composites of carbon nanotubes loaded with Ag and TiO2 nanoparticle for use as anode material in lithium-ion batteries. Electrochimica Acta, 2008, 53, 6351-6355. | 5.2 | 73 |
| 138 | Electrochemical performance of arc-produced carbon nanotubes as anode material for lithium-ion batteries. Electrochimica Acta, 2007, 52, 5286-5293. | 5.2 | 79 |
| 139 | Nanosized tin and tin oxides loaded expanded mesocarbon microbeads as negative electrode material for lithium-ion batteries. Journal of Power Sources, 2007, 173, 487-494. | 7.8 | 44 |
| 140 | Electrochemical performance of expanded mesocarbon microbeads as anode material for lithium-ion batteries. Electrochemistry Communications, 2006, 8, 137-142. | 4.7 | 279 |
| 141 | Expansion of mesocarbon microbeads. Carbon, 2006, 44, 730-733. | 10.3 | 14 |